AMERICAN SOCIETY FOR MICROBIOLOGY | Antimicrobial Agents and Chemotherapy®

ANTIVIRAL AGENTS

The Myxobacterial Metabolite Soraphen A Inhibits HIV-1 by Reducing Virus Production and Altering Virion Composition

Eric Fleta-Soriano,[a] Katarína Smutná,[a] Javier P. Martínez,[a] Cristina Lorca Oró,[b] S. Kashif Sadiq,[a] Gilles Mirambeau,[b] Carmen Lopez-Iglesias,[c] Marta Bosch,[d] Albert Pol,[d,g] Mark Brönstrup,[e] Juana Diez,[f] Andreas Meyerhans[a,g]

Infection Biology Group, DCEXS, Universitat Pompeu Fabra, Barcelona, Spain[a]; AIDS Research Group, IDIBAPS, Barcelona, Spain[b]; Cryo-Electron Microscopy Unit, CCiTUB, Universitat de Barcelona, Barcelona, Spain[c]; Cell Compartments and Signaling Group, Institut d'Investigacions Biomèdiques August Pi i Sunyer (IDIBAPS), Barcelona, Spain[d]; Department of Chemical Biology, Helmholtz Centre for Infection Research, Braunschweig, Germany[e]; Molecular Virology Group, DCEXS, Universitat Pompeu Fabra, Barcelona, Spain[f]; Institució Catalana de Recerca i Estudis Avançats (ICREA), Barcelona, Spain[g]

ABSTRACT Soraphen A is a myxobacterial metabolite that blocks the acetyl-coenzyme A carboxylase of the host and was previously identified as a novel HIV inhibitor. Here, we report that soraphen A acts by reducing virus production and altering the gp120 virion content, impacting entry capacity and infectivity. These effects are partially reversed by addition of palmitic acid, suggesting that inhibition of HIV envelope palmitoylation is one of the mechanisms of antiviral action.

KEYWORDS soraphen A, HIV, fatty acid synthesis, host factor, broad-spectrum antiviral, human immunodeficiency virus

Received 7 April 2017 **Returned for modification** 3 May 2017 **Accepted** 18 May 2017

Accepted manuscript posted online 22 May 2017

Citation Fleta-Soriano E, Smutná K, Martínez JP, Lorca Oró C, Sadiq SK, Mirambeau G, Lopez-Iglesias C, Bosch M, Pol A, Brönstrup M, Diez J, Meyerhans A. 2017. The myxobacterial metabolite soraphen A inhibits HIV-1 by reducing virus production and altering virion composition. Antimicrob Agents Chemother 61:e00739-17. https://doi.org/10.1128/AAC.00739-17.

Address correspondence to Javier P. Martínez, javier.martinez@upf.edu, or Andreas Meyerhans, andreas.meyerhans@upf.edu.

E.F.-S. and K.S. contributed equally to this work.

Cellular lipids play an important role in the propagation of diverse viruses (1). A key pathway in lipid metabolism is *de novo* fatty acid synthesis mediated by acetyl-coenzyme A carboxylase (ACC) and multifunctional fatty acid synthase. Blockage of these enzymes by small molecules leads to broad-spectrum inhibition of several viruses, including hepatitis C virus (HCV), West Nile virus, dengue virus, yellow fever virus, rotavirus, human cytomegalovirus, vesicular stomatitis virus, and influenza virus (2–7). A highly potent inhibitor of ACC is soraphen A (SorA), a myxobacterial secondary metabolite that we previously identified as an HIV inhibitor in an antiviral screening assay (8) and recently showed to efficiently inhibit HCV with a large therapeutic window (9). Here, we sought to further determine the anti-HIV properties of SorA.

To analyze the antiviral potency of SorA, TZM-bl cells or primary peripheral blood mononuclear cells (PBMCs) were infected with HIV_{LAI} and HIV_{BaL} wild-type strains and with a primary HIV isolate from clade A under increasing SorA concentrations (Fig. 1A to D). The production of infectious virus was then tested by titrating the culture supernatants on TZM-bl cells with a luciferase readout (10, 11). The effect of SorA on cell viability was assessed in parallel by a commercial ATP assay. SorA reduced infectious virus production in a dose-dependent manner. The calculated 50% effective concentration (EC_{50}) ranged from ~0.2 to 2 μM, depending on the cells and virus used. No SorA-mediated toxicity was detected up to the 50 μM concentration tested.

The inhibitory effect of SorA was verified by p24 intracellular immunostaining of lymphoid MT-2 cells infected with HIV-1_{LAI} in the presence or absence of SorA or the ACC inhibitor 5-(tetradecyloxy)-2-furoic acid (TOFA) as control (Fig. 1E to H). SorA reduced p24 production compared with the dimethyl sulfoxide (DMSO) control but did not completely abolish it (Fig. 1G, left panel). No p24 was detected when fresh cells

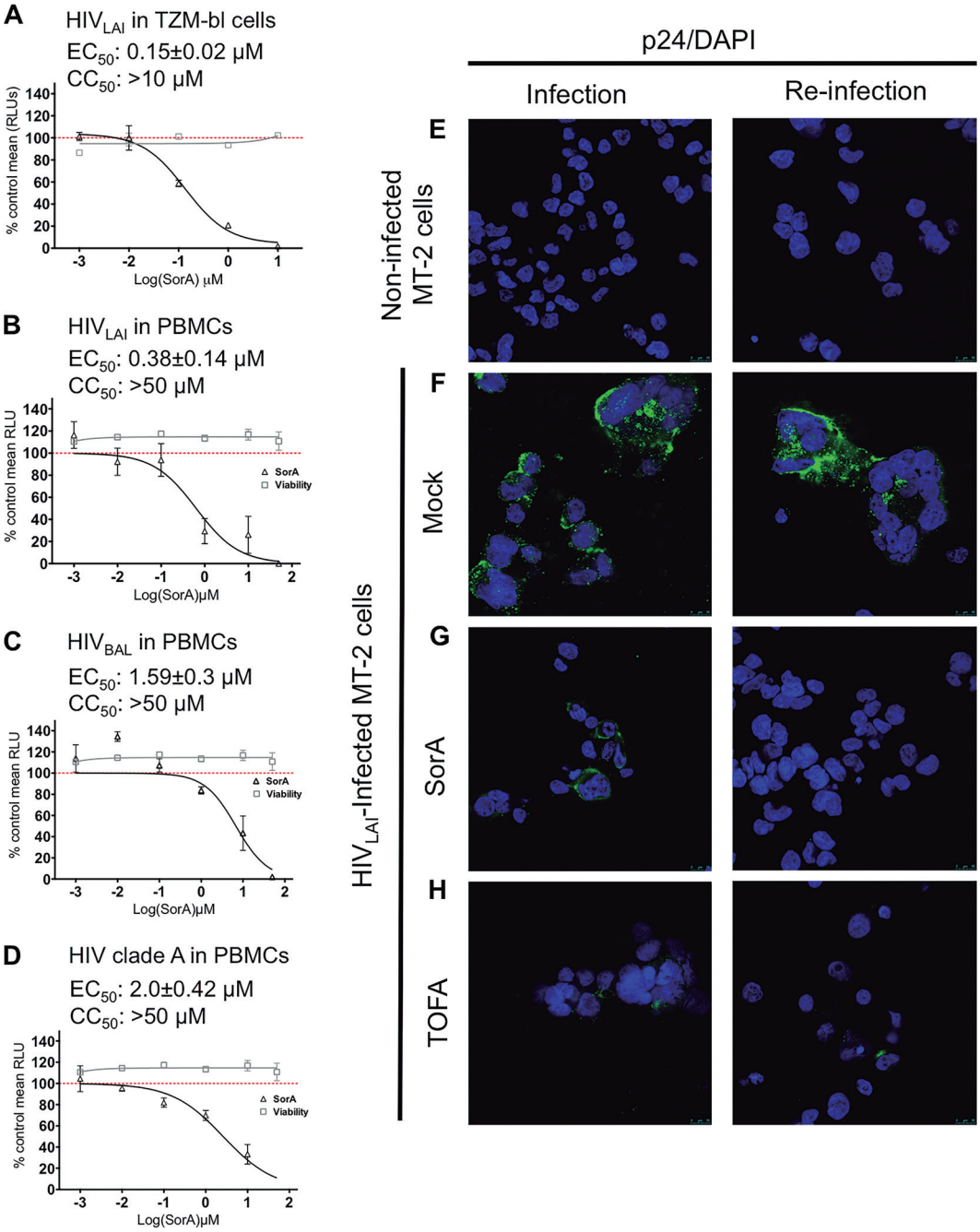

FIG 1 Soraphen A inhibits infectious HIV production. TZM-bl cells or PBMCs were seeded in 96-well plates and treated with increasing concentrations of SorA in triplicate. TZM-bl cells (A) or PBMCs (B to D) were infected with HIV-1$_{LAI}$ (A, $n = 5$; B, $n = 4$), HIV-1$_{BaL}$ (C; $n = 5$), or a primary isolate of HIV-1 KER2018 (D; $n = 3$) at a multiplicity of infection of 0.5. Supernatants were used to reinfect new TZM-bl cells. A representative curve is shown in every case. Infection (triangles) and cell viability (squares) are marked. The mean relative light units (RLU) are plotted as percentage relative to the DMSO control (vehicle). Error bars, standard error of the mean; CC$_{50}$, 50% cytotoxic concentration. (E to H) MT-2 cells were spinoculated with HIV$_{LAI}$ and treated with SorA or TOFA as control. At 48 h after infection, supernatants were collected and used to infect new MT-2 cells, while cells were fixed and stained for HIV-p24 protein (green signals) and with 4′,6-diamidino-2-phenylindole (DAPI) (blue signals) (left panels). Newly infected MT-2 cells were then analyzed in the same manner (right panels). Noninfected MT-2 cells (E) and infected but untreated MT-2 cells (F) were used as negative and positive controls, respectively.

were incubated with supernatants from SorA-treated infected cells, thus confirming that the inhibitory effect occurs mainly on late processes in the HIV-1 life cycle (Fig. 1G, right panel). These results are consistent with our prior work, which first demonstrated the anti-HIV effect of SorA (8).

An altered lipid content of cells may change membrane composition and fluidity, which in turn may interfere with the reorganization of HIV structural proteins during viral maturation (12, 13). To test this, the cholesterol content and fluidity of SorA-treated Jurkat T cell membranes and PBMC membranes were analyzed by flow cytometry using the cholesterol-binding antibiotic filipin and the fluorescent membrane-partitioning dye di-4-ANEPPDHQ, respectively (14, 15). In the latter, the fluorescence emission is sensitive to the membrane order of its local molecular environment (16, 17) (for details, see the supplemental material). For both assays, cyclodextrin, which leads to cholesterol depletion and increased fluidity of membranes, was used as a positive control. Neither the cholesterol content (see Fig. S1A in the supplemental material) nor the membrane fluidity (Fig. S1B and C) changed significantly after SorA treatment. To test whether maturation of HIV particles is inhibited by SorA, latently HIV-1-infected ACH2 cells cultured in the presence of the drug were activated with the histone deacetylase inhibitor vorinostat to produce virus. Forty-eight hours after activation, cells were fixed with glutaraldehyde, stained with osmium tetroxide, and analyzed by transmission electron microscopy (TEM). More than 500 viral particles per condition were counted by TEM and classified as mature, immature, or undetermined (Fig. 2A to D). The HIV protease inhibitor lopinavir (LPN) was used as a positive control. As shown in Fig. 2E, ~90% of viruses were mature in SorA-treated samples, a number similar to that for the DMSO control. In contrast, ~90% of viral particles were immature in the LPN control.

Because the SorA effect occurs during late steps of the HIV replication cycle but does not influence maturation, we analyzed the CD4 receptor binding and membrane fusion capacity of viruses produced from SorA-treated cells. For the first experiment, we made use of the property of HIV particles to bind CD4 but not fuse or enter when exposed to target cells at 4°C (18). Briefly, TZM-bl cells were spinoculated for 30 min at 4°C with 10 ng p24-containing supernatants obtained from activated ACH2 cells in the presence or absence of SorA. Cells were then washed and lysed, and the viral p24 was quantified by enzyme-linked immunosorbent assay (ELISA). As shown in Fig. 2F, CD4 binding of viruses produced from ACH2 cells in the presence of SorA was reduced by 50%. To determine the capacity of viruses to fuse to the target cells, we used an enzyme-based HIV-1 fusion assay (19). Jurkat cells were infected with equal p24 amounts of HIV pseudoparticles containing a Vpr-BlaM fusion protein produced in the presence of SorA or LPN. Samples were incubated at 37°C to allow for viral fusion and loaded with CCF2-AM, the substrate for β-lactamase. The fusion inhibitor enfuvirtide (T20) was used as a positive control. Samples were incubated overnight, analyzed by flow cytometry, and used to estimate fusion capacity as described previously (19). As shown in Fig. 2G (and Fig. S2 in the supplemental material), we observed a >60% membrane fusion reduction of HIV particles generated in the presence of SorA. Given that the effect of SorA in reducing virus entry was not due to a defect in maturation, we next determined the relative amounts of p24 and gp120 in viral particles produced in the presence of the drug. For this, p24 and gp120 amounts in virus-containing supernatants from activated ACH2 cells and from PBMCs infected with HIV_{LAI} in the presence or absence of SorA or DMSO as control were quantified by ELISA. As shown in Fig. 2H, SorA reduced the content of both proteins compared with the DMSO control. For p24, the relative reduction was ~50%. The effect was more pronounced for gp120 than for p24, with 80% and 60% reduction, respectively. To exclude a SorA-mediated effect on global HIV transcription, we next performed quantitative PCR in both SorA-treated infected cells and virus-containing supernatants. Compared with treatment with the DMSO control, SorA treatment reduced HIV RNA in virus-containing supernatants but not in infected cells (see Fig. S3 in the supplemental material). Together, these results suggest an overall drug-induced alteration in virion composition that results in loss of infectivity.

Inhibition of *de novo* fatty acid synthesis leads to a reduction of palmitic acid (PA), which is the end product of this pathway (2, 20). As the HIV-1 envelope (Env) is commonly palmitoylated at cysteine amino acids C764 and C837 in the C-terminal tail of gp41 (21), we hypothesized that PA addition to the culture medium would recover

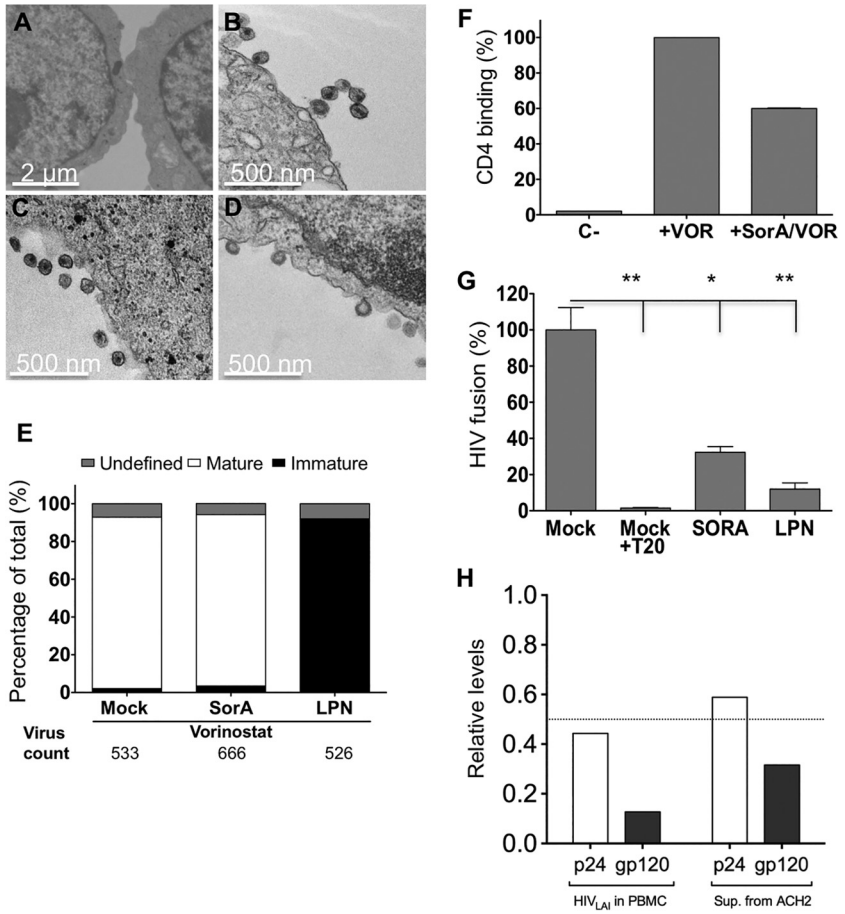

FIG 2 Soraphen A does not impair virion maturation but affects binding to CD4 and membrane fusion to target cells. (A to D) ACH2 cells were activated with vorinostat (VOR) and treated with SorA 10 μM, lopinavir (LPN) 10 μM or DMSO (mock). Cells were fixed and processed for transmission electron microscopy (TEM) 48 h after infection. TEM pictures were taken of untreated ACH2 cells (A) and those treated with Vor+DMSO (B), Vor+SorA (C), and Vor+LPN (D). (E) The numbers of mature, immature, and unclassified viral particles are shown. (F) Normalized CD4 binding is represented ($n = 2$). Mock-treated activated ACH2 cells and nonactivated ACH2 cells were used as controls. (G) HIV pseudoparticles containing a Vpr-BlaM fusion protein were produced from transfected 293T cells in the presence of SorA 10 μM, LPN 10 μM, or DMSO (mock) and used to infect Jurkat cells by spinoculation. Normalized HIV fusion values are shown ($n = 5$; *, $P < 0.05$; **, $P < 0.01$). (H) Levels of p24 and gp120 relative to DMSO control (set to 1) are shown. The dotted line highlights the half relative level. Single concentrations of compounds were chosen based on inhibitory extent and lack of toxicity.

the infectivity of viruses produced from SorA-treated cells. To test this, several HIV-1 pseudoviruses (HIVpp) with variations in the number of palmitoylation sites in the Env were generated in HEK 293T cells in the presence or absence of SorA with or without the addition of PA. The HIV NL4.3-derived backbone plasmid pNLE-ΔEnv was cotransfected with HIV-1Env expression plasmids carrying two (pHXB2 and pW61D_TCLA.71), one (pWITO4160 and pSS1196.1), or no (pBal.26 and pMN.3) palmitoylation sites (22). At 48 h after transfection, supernatants were clarified by centrifugation and pelleted in a sucrose buffer, as described previously (23), to minimize the presence of non-particle-associated antigens. Virus-containing pellets were analyzed for p24 and gp120 content by Western blot and for infectivity in TZM-bl cells. The relative values with respect to the produced HIVpp without SorA addition are given in Fig. 3. SorA inhibited the infectivity (Fig. 3A) and reduced the p24 (Fig. 3B) and gp120 (Fig. 3C) content in all virus-containing samples. Addition of PA partially restored the inhibitory effect of SorA (Fig. 3A to C, black bars). The recovery in infectivity (Fig. 3D) and gp120 levels (Fig. 3F) seemed to depend on the number of palmitoylation sites, being highest when two such sites were present in the Env. For p24, the recovery effect was less evident

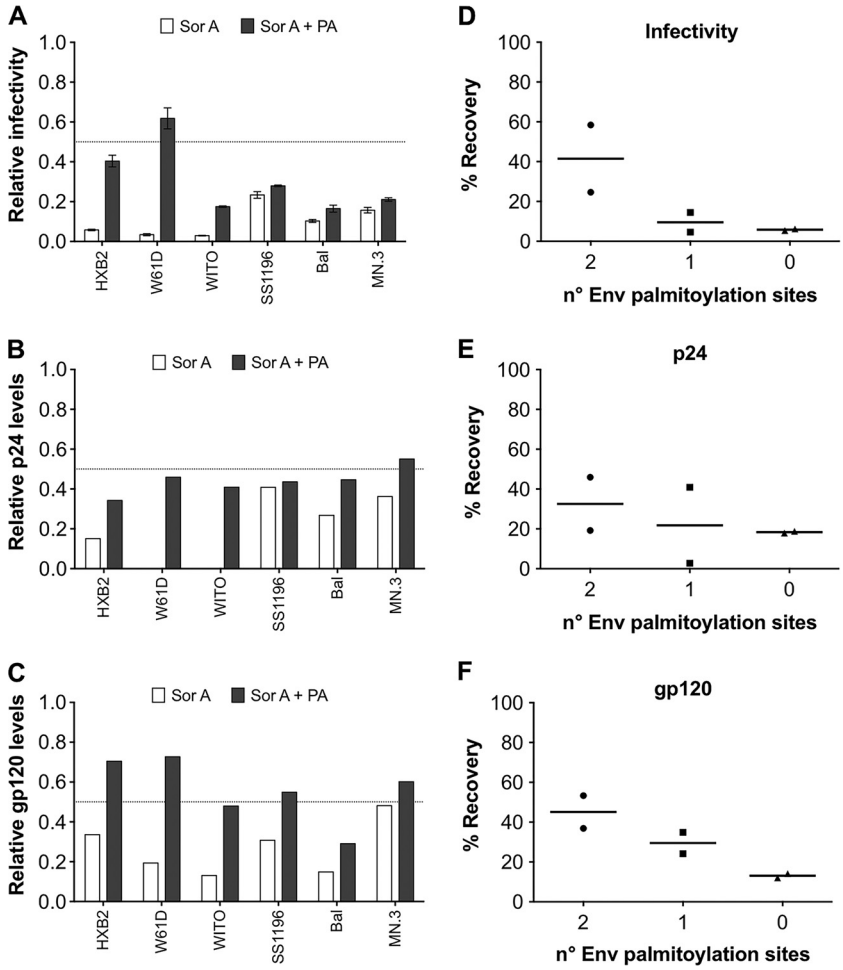

FIG 3 Palmitic acid (PA) restores the SorA-mediated inhibition of infectious HIV production. Effect of SorA on produced HIVpp infectivity (A), p24 content (B), and gp120 content (C) (white bars) and the respective recovery by PA addition (black bars). HIVpp with Env proteins that carry mutations in the gp41 palmitoylation sites Cys764/Cys837 were produced from 293T cells in the presence of SorA 10 μM or DMSO control (vehicle) and tested for infectivity and p24 and gp120 content. Reductions and recovery levels by PA addition are shown as normalized values relative to the DMSO or DMSO+PA controls, respectively. The Env proteins of the HIVpp differ in the number of palmitoylation sites at residues 764/837 and have the following features: Cys764/Cys837 in HXB2 and W61D, Cys764/no Cys837 in WITO, no Cys764/Cys837 in SS1196, and no Cys764/no Cys837 in BaL and MN.3. The percent recovery was calculated by subtracting the mean infectivity (from three independent experiments), p24 values, or gp120 values of samples not treated with PA from the values of the samples treated with PA for each virus. The percentages of PA-mediated recovery of virus infectivity (D), p24 (E), and gp120 (F) related to the number of palmitoylation sites are shown. The dotted lines highlight half relative levels. Values for B and C are derived from Western blot quantification of p24 and gp120, respectively. Single concentrations of compounds were chosen based on inhibitory extent and lack of toxicity.

(Fig. 3E). Although the values obtained did not reach statistical significance under the conditions tested, the observed tendency suggested that the SorA-mediated reduction in virus infectivity was mechanistically linked to a defect in Env palmitoylation.

The role of palmitoylation in HIV infectivity remains controversial. While Rousso et al. (24) defined Env palmitoylation as critical for HIV infectivity and Bhattacharya et al. (25) showed a 60% to 90% infectivity reduction of virus mutants that cannot be palmitoylated, data by Chan et al. (26) suggest that palmitoylation does not affect HIV-1 infectivity. The explanation for this discrepancy is likely within the experimental details of the different test systems and virus constructs used that may directly affect Env densities on viral particles and thus virus infectivity and palmitoylation dependency. The cytoplasmic tail of gp41 that harbors the palmitoylation sites and the Gag matrix domain within Gag plus several host cell components are important players in Env

incorporation into the virion (27, 28). Env density then can affect virus infectivity (29); however, this is predicted to vary among HIV strains that exhibit different entry stoichiometries requiring between 1 and 7 Env trimers to complete the infection process (30). Thus, a number of effects may mask a reduction in infectivity due to a lack of Env palmitoylation. Nonetheless, the HIV-1 Env palmitoylation sites are highly conserved among different virus strains, suggesting their functional importance in HIV-1 propagation. The data presented here seem to reinforce this notion.

In summary, SorA exhibits multiple inhibitory effects on the HIV life cycle at low micromolar concentrations. Its ability to inhibit with high potency a key element of the *de novo* fatty acid synthesis pathway that is critical for the efficient expansion of many different viruses and its low toxicity for eukaryotic cells make SorA an attractive starting point for the development of a broad-spectrum antiviral drug (31). Further studies with SorA derivatives are envisioned.

SUPPLEMENTAL MATERIAL

Supplemental material for this article may be found at https://doi.org/10.1128/AAC.00739-17.

SUPPLEMENTAL FILE 1, PDF file, 0.3 MB.

ACKNOWLEDGMENTS

The research is supported by FPI grants (BES-2011-048569 to E. Fleta-Soriano, SAF2013-46077-R and SAF2016-75505-R to J. P. Martínez and A. Meyerhans, and BFU2016-80039-R to J. Diez) from the Spanish Ministry of Economy, Industry and Competitiveness; FEDER (AEI/MINEICO/FEDER, UE), the "Maria de Maeztu" Programme for Units of Excellence in R&D (MDM-2014-0370); and the German Centre for Infection Research (DZIF, to M. Brönstrup).

The funders had no role in the study design, data collection and interpretation, or decision to submit the work for publication.

REFERENCES

1. Heaton NS, Randall G. 2011. Multifaceted roles for lipids in viral infection. Trends Microbiol 19:368–375. https://doi.org/10.1016/j.tim.2011.03.007.
2. Martin-Acebes MA, Blazquez AB, Jimenez de Oya N, Escribano-Romero E, Saiz JC. 2011. West Nile virus replication requires fatty acid synthesis but is independent on phosphatidylinositol-4-phosphate lipids. PLoS One 6:e24970. https://doi.org/10.1371/journal.pone.0024970.
3. Munger J, Bennett BD, Parikh A, Feng XJ, McArdle J, Rabitz HA, Shenk T, Rabinowitz JD. 2008. Systems-level metabolic flux profiling identifies fatty acid synthesis as a target for antiviral therapy. Nat Biotechnol 26:1179–1186. https://doi.org/10.1038/nbt.1500.
4. Schlesinger MJ, Malfer C. 1982. Cerulenin blocks fatty acid acylation of glycoproteins and inhibits vesicular stomatitis and Sindbis virus particle formation. J Biol Chem 257:9887–9890.
5. Nasheri N, Joyce M, Rouleau Y, Yang P, Yao S, Tyrrell DL, Pezacki JP. 2013. Modulation of fatty acid synthase enzyme activity and expression during hepatitis C virus replication. Chem Biol 20:570–582. https://doi.org/10.1016/j.chembiol.2013.03.014.
6. Heaton NS, Perera R, Berger KL, Khadka S, Lacount DJ, Kuhn RJ, Randall G. 2010. Dengue virus nonstructural protein 3 redistributes fatty acid synthase to sites of viral replication and increases cellular fatty acid synthesis. Proc Natl Acad Sci U S A 107:17345–17350. https://doi.org/10.1073/pnas.1010811107.
7. Gaunt ER, Cheung W, Richards JE, Lever A, Desselberger U. 2013. Inhibition of rotavirus replication by downregulation of fatty acid synthesis. J Gen Virol 94:1310–1317. https://doi.org/10.1099/vir.0.050146-0.
8. Martinez JP, Hinkelmann B, Fleta-Soriano E, Steinmetz H, Jansen R, Diez J, Frank R, Sasse F, Meyerhans A. 2013. Identification of myxobacteria-derived HIV inhibitors by a high-throughput two-step infectivity assay. Microb Cell Fact 12:85. https://doi.org/10.1186/1475-2859-12-85.
9. Koutsoudakis G, Romero-Brey I, Berger C, Perez-Vilaro G, Perin PM, Vondran FW, Kalesse M, Harmrolfs K, Muller R, Martinez JP, Pietschmann T, Bartenschlager R, Bronstrup M, Meyerhans A, Diez J. 2015. Soraphen A: a broad-spectrum antiviral natural product with potent anti-hepatitis C virus activity. J Hepatol 63:813–821. https://doi.org/10.1016/j.jhep.2015.06.002.
10. Montefiori DC. 2005. Evaluating neutralizing antibodies against HIV, SIV, and SHIV in luciferase reporter gene assays. Curr Protoc Immunol Chapter 12:Unit 12.11. https://doi.org/10.1002/0471142735.im1211s64.
11. Wei X, Decker JM, Liu H, Zhang Z, Arani RB, Kilby JM, Saag MS, Wu X, Shaw GM, Kappes JC. 2002. Emergence of resistant human immunodeficiency virus type 1 in patients receiving fusion inhibitor (T-20) monotherapy. Antimicrob Agents Chemother 46:1896–1905. https://doi.org/10.1128/AAC.46.6.1896-1905.2002.
12. Aloia RC, Tian H, Jensen FC. 1993. Lipid composition and fluidity of the human immunodeficiency virus envelope and host cell plasma membranes. Proc Natl Acad Sci U S A 90:5181–5185. https://doi.org/10.1073/pnas.90.11.5181.
13. Chojnacki J, Staudt T, Glass B, Bingen P, Engelhardt J, Anders M, Schneider J, Muller B, Hell SW, Krausslich HG. 2012. Maturation-dependent HIV-1 surface protein redistribution revealed by fluorescence nanoscopy. Science 338:524–528. https://doi.org/10.1126/science.1226359.
14. Ingelmo-Torres M, Gaus K, Herms A, Gonzalez-Moreno E, Kassan A, Bosch M, Grewal T, Tebar F, Enrich C, Pol A. 2009. Triton X-100 promotes a cholesterol-dependent condensation of the plasma membrane. Biochem J 420:373–381. https://doi.org/10.1042/BJ20090051.
15. Muller CP, Stephany DA, Winkler DF, Hoeg JM, Demosky SJ, Jr, Wunderlich JR. 1984. Filipin as a flow microfluorometry probe for cellular cholesterol. Cytometry 5:42–54. https://doi.org/10.1002/cyto.990050108.
16. Bosch M, Mari M, Herms A, Fernandez A, Fajardo A, Kassan A, Giralt A, Colell A, Balgoma D, Barbero E, Gonzalez-Moreno E, Matias N, Tebar F, Balsinde J, Camps M, Enrich C, Gross SP, Garcia-Ruiz C, Perez-Navarro E, Fernandez-Checa JC, Pol A. 2011. Caveolin-1 deficiency causes cholesterol-dependent mitochondrial dysfunction and apoptotic susceptibility. Curr Biol 21:681–686. https://doi.org/10.1016/j.cub.2011.03.030.
17. Owen DM, Gaus K. 2010. Optimized time-gated generalized polarization imaging of Laurdan and di-4-ANEPPDHQ for membrane order image

contrast enhancement. Microsc Res Tech 73:618–622. https://doi.org/10.1002/jemt.20801.
18. Melikyan GB, Markosyan RM, Hemmati H, Delmedico MK, Lambert DM, Cohen FS. 2000. Evidence that the transition of HIV-1 Gp41 into a six-helix bundle, not the bundle configuration, induces membrane fusion. J Cell Biol 151:413–424. https://doi.org/10.1083/jcb.151.2.413.
19. Cavrois M, De Noronha C, Greene WC. 2002. A sensitive and specific enzyme-based assay detecting HIV-1 virion fusion in primary T lymphocytes. Nat Biotechnol 20:1151–1154. https://doi.org/10.1038/nbt745.
20. Jump DB, Torres-Gonzalez M, Olson LK. 2011. Soraphen A, an inhibitor of acetyl CoA carboxylase activity, interferes with fatty acid elongation. Biochem Pharmacol 81:649–660. https://doi.org/10.1016/j.bcp.2010.12.014.
21. Yang C, Spies CP, Compans RW. 1995. The human and simian immunodeficiency virus envelope glycoprotein transmembrane subunits are palmitoylated. Proc Natl Acad Sci U S A 92:9871–9875. https://doi.org/10.1073/pnas.92.21.9871.
22. Tsunetsugu-Yokota Y, Kobayahi-Ishihara M, Wada Y, Terahara K, Takeyama H, Kawana-Tachikawa A, Tokunaga K, Yamagishi M, Martinez JP, Meyerhans A. 2016. Homeostatically maintained resting naive CD4+ T cells resist latent HIV reactivation. Front Microbiol 7:1944.
23. Jiang W, Hua R, Wei M, Li C, Qiu Z, Yang X, Zhang C. 2015. An optimized method for high-titer lentivirus preparations without ultracentrifugation. Sci Rep 5:13875. https://doi.org/10.1038/srep13875.
24. Rousso I, Mixon MB, Chen BK, Kim PS. 2000. Palmitoylation of the HIV-1 envelope glycoprotein is critical for viral infectivity. Proc Natl Acad Sci U S A 97:13523–13525. https://doi.org/10.1073/pnas.240459697.
25. Bhattacharya J, Peters PJ, Clapham PR. 2004. Human immunodeficiency virus type 1 envelope glycoproteins that lack cytoplasmic domain cysteines: impact on association with membrane lipid rafts and incorporation onto budding virus particles. J Virol 78:5500–5506. https://doi.org/10.1128/JVI.78.10.5500-5506.2004.
26. Chan WE, Lin HH, Chen SS. 2005. Wild-type-like viral replication potential of human immunodeficiency virus type 1 envelope mutants lacking palmitoylation signals. J Virol 79:8374–8387. https://doi.org/10.1128/JVI.79.13.8374-8387.2005.
27. Da Silva ES, Mulinge M, Bercoff DP. 2013. The frantic play of the concealed HIV envelope cytoplasmic tail. Retrovirology 10:54. https://doi.org/10.1186/1742-4690-10-54.
28. Tedbury PR, Freed EO. 2014. The role of matrix in HIV-1 envelope glycoprotein incorporation. Trends Microbiol 22:372–378. https://doi.org/10.1016/j.tim.2014.04.012.
29. Bachrach E, Dreja H, Lin Y-L, Mettling C, Pinet V, Corbeau P, Piechaczyk M. 2005. Effects of virion surface gp120 density on infection by HIV-1 and viral production by infected cells. Virology 332:418–429. https://doi.org/10.1016/j.virol.2004.11.031.
30. Brandenberg OF, Magnus C, Rusert P, Regoes RR, Trkola A. 2015. Different infectivity of HIV-1 strains is linked to number of envelope trimers required for entry. PLoS Pathog 11:e1004595. https://doi.org/10.1371/journal.ppat.1004595.
31. Shen Y, Volrath SL, Weatherly SC, Elich TD, Tong L. 2004. A mechanism for the potent inhibition of eukaryotic acetyl-coenzyme A carboxylase by soraphen A, a macrocyclic polyketide natural product. Mol Cell 16:881–891. https://doi.org/10.1016/j.molcel.2004.11.034.